Mitochondrial DNA, morphology, and the phylogenetic relationships of Antarctic icefishes (Notothenioidei: Channichthyidae)

Thomas J. Near,[a,*] James J. Pesavento,[b] and Chi-Hing C. Cheng[b]

[a] *Center for Population Biology, One Shields Avenue, University of California, Davis, CA 95616, USA*
[b] *Department of Animal Biology, 515 Morrill Hall, University of Illinois, Urbana, IL 61801, USA*

Abstract

The Channichthyidae is a lineage of 16 species in the Notothenioidei, a clade of fishes that dominate Antarctic near-shore marine ecosystems with respect to both diversity and biomass. Among four published studies investigating channichthyid phylogeny, no two have produced the same tree topology, and no published study has investigated the degree of phylogenetic incongruence between existing molecular and morphological datasets. In this investigation we present an analysis of channichthyid phylogeny using complete gene sequences from two mitochondrial genes (ND2 and 16S) sampled from all recognized species in the clade. In addition, we have scored all 58 unique morphological characters used in three previous analyses of channichthyid phylogenetic relationships. Data partitions were analyzed separately to assess the amount of phylogenetic resolution provided by each dataset, and phylogenetic incongruence among data partitions was investigated using incongruence length difference (ILD) tests. We utilized a parsimony-based version of the Shimodaira–Hasegawa test to determine if alternative tree topologies are significantly different from trees resulting from maximum parsimony analysis of the combined partition dataset. Our results demonstrate that the greatest phylogenetic resolution is achieved when all molecular and morphological data partitions are combined into a single maximum parsimony analysis. Also, marginal to insignificant incongruence was detected among data partitions using the ILD. Maximum parsimony analysis of all data partitions combined results in a single tree, and is a unique hypothesis of phylogenetic relationships in the Channichthyidae. In particular, this hypothesis resolves the phylogenetic relationships of at least two species (*Channichthys rhinoceratus* and *Chaenocephalus aceratus*), for which there was no consensus among the previous phylogenetic hypotheses. The combined data partition dataset provides substantial statistical power to discriminate among alternative hypotheses of channichthyid relationships. These findings suggest the optimal strategy for investigating the phylogenetic relationships of channichthyids is one that uses all available phylogenetic data in analyses of combined data partitions.
© 2003 Elsevier Science (USA). All rights reserved.

1. Introduction

The ichthyofauna of the Southern Ocean surrounding Antarctica is dominated both in diversity and biomass by a monophyletic lineage of fishes, the Notothenioidei (Eastman, 1993). There are approximately 130 notothenioid species classified in eight families (Eastman and Eakin, 2000). Many of these species are endemic to High Antarctic near-shore habitats at subzero temperatures, and exhibit several morphological, physiological, and biochemical adaptations to these extreme environments (Eastman, 1993; Kock, 1992). Notothenioid fishes are ecologically diverse, and have been hypothesized to represent an adaptive radiation in the coastal Antarctic regions of the Southern Ocean (Clarke and Johnston, 1996).

One of the most interesting notothenioid lineages is the Channichthyidae, or icefishes, a clade that contains 16 recognized species (Eastman and Eakin, 2000; Iwami and Kock, 1990; La Mesa et al., 2002). Most channichthyid species are confined to the Antarctic region, but at least three species are found outside of this region in the Kerguelen Islands and the Falkland Islands

* Corresponding author. Fax: +1-530-752-1449.
E-mail address: tjnear@ucdavis.edu (T.J. Near).

(Iwami and Kock, 1990). Channichthyids are well-known for being the only group of vertebrates that lack oxygen-transporting hemoglobin in the blood. The cardiovascular system of channichthyids is thought to have compensated for the lack of hemoglobin and the low oxygen-carrying capacity of the blood through adaptations that include a greater blood volume and higher cardiac output when compared to other notothenioids (Hemmingsen, 1991). The external morphology of channichthyids reflects their role as predators of fish and epibenthic crustaceans. The snout is broad and spatulate, and the mouth is large with small teeth that may facilitate grasping prey. The mouth is not protrusible and is thought to reflect a mode of prey capture that involves feeding on organisms in the water column, as opposed to most other notothenioids that use a protrusible mouth to grasp benthic organisms off of the bottom (Iwami, 1985). Channichthyids have been cited as an example of paedeomorphic evolution (Voskoboinikova, 2001), because larval and juvenile features such as weakly ossified cartilaginous skeletons are retained into adulthood.

Phylogenetic analysis of morphology and DNA sequence data agree that channichthyids are a monophyletic group, and are one of the most derived clades of notothenioids (Balushkin, 2000; Bargelloni et al., 2000; Iwami, 1985). Phylogenetic hypotheses inferred from morphology places the notothenioid family Bathydraconidae as the sister lineage of the Channichthyidae (Balushkin, 2000; Eakin, 1981; Iwami, 1985). Phylogenetic analyses of mt rRNA sequences results in an hypothesis that the channichthyids are monophyletic and nested in a paraphyletic Bathydraconidae (Bargelloni et al., 2000).

Phylogenetic relationships within Channichthyidae have been investigated using both discretely coded morphological characters (Balushkin, 2000; Iwami, 1985; Voskoboinikova, 2000) and mtDNA sequence data (Chen et al., 1998). Among the three published hypotheses of channichthyid phylogeny resulting from analyses of morphological characters, two are highly congruent and substantially different from the third (Fig. 1). Iwami (1985) and Voskoboinikova (2000) place *Champsocephalus* as basal and the sister taxon of all other channichthyids (Fig. 1). In contrast, Balushkin (2000) places the Kerguelen endemic *Channichthys rhinoceratus* as basal and the sister taxon of the remaining channichthyids (Fig. 1), while Iwami (1985) and Voskoboinikova (2000) propose that *Channichthys rhinoceratus* is phylogenetically derived within the clade. All three of the morphology inferred hypotheses disagree on the phylogenetic relationships of the genera *Cryodraco* and *Chaenocephalus* (Fig. 1). Two areas of agreement among these three hypotheses are the monophyletic clade containing the genera *Pagetopsis*, *Pseudochaenichthys*, and *Neopagetopsis*, and a sister taxon relationship between *Chaenodraco* and *Chionodraco* (Fig. 1). In Iwami's (1985) hypothesis the phylogenetic position of *Dacodraco hunteri* is unresolved, presumably due to missing character data for this taxon, while both Voskoboinikova (2000) and Balushkin (2000) present hypotheses that resolve the phylogenetic relationships of *Dacodraco hunteri* (Fig. 1).
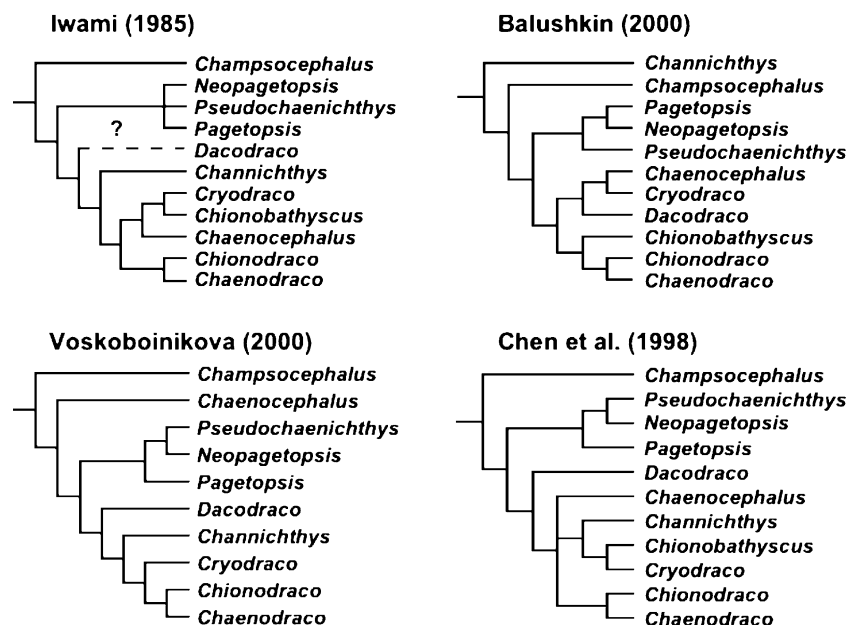

Fig. 1. Previous hypotheses of relationships among channichthyid genera.

Partial mtDNA gene sequences from the control region and cytochrome *b* have been used to investigate phylogenetic relationships for 14 channichthyid species and a single outgroup species from the Bathydraconidae (Chen et al., 1998). Maximum parsimony (MP) analysis of the mtDNA data results in two most-parsimonious trees that differ only in the placement of *Chaenocephalus aceratus* (Chen et al., 1998). The strict consensus of these two trees is very similar to the morphological inferred hypotheses of Iwami (1985) and Voskoboinikova (2000) (Fig. 1). In fact, Chen et al. (1998) point out that MP analysis of Iwami's (1985) character matrix yields four most-parsimonious trees, of which the strict consensus is much less resolved than the hypothesis (Fig. 1) presented in Iwami (1985). The trees recovered from MP analysis of the mtDNA sequence data are identical to two of the four trees recovered from MP analysis of Iwami's (1985) morphological data (Chen et al., 1998). As a result, Chen et al. (1998) conclude that there is no incongruence between the mtDNA and Iwami's (1985) morphological datasets.

The differences in tree topology among the four published phylogenetic analyses of channichthyids indicate potential phylogenetic incongruence among the datasets used to generate these hypotheses. The generation of different trees from each of the four separate datasets results in uncertainty with regard to which phylogenetic hypothesis to use in studying the evolutionary diversification of this clade. Our goal was to investigate potential phylogenetic incongruence between partitions of morphological and molecular characters in the Channichthyidae. In particular, we are interested in developing hypotheses of channichthyid relationships that explain all of the available phylogenetic information, as well as providing the greatest phylogenetic resolution and discrimination of alternative phylogenetic hypotheses. The molecular data partitions we used contain two complete mitochondrial genes (ND2 and 16S rRNA) sampled from all 16 recognized channichthyid species, and several bathydraconid species to serve as outgroup taxa. All unique characters used to infer relationships of channichthyids among the three published morphological phylogenetic studies were collected into a single coded data matrix. With a combined dataset containing all partitions of molecular and morphological characters, we attempt to assess phylogenetic congruence between the individual mtDNA genes, and congruence between mtDNA characters and morphological characters. By combining molecular and morphological data partitions, we investigate the effects of such combinations on the degree of phylogenetic resolution in resulting phylogenetic hypotheses of the Channichthyidae. Also, the phylogenetic hypothesis resulting from the combined data partition analysis is compared to previous hypotheses of relationships using a unique parsimony-based Shimodaira–Hasegawa (SH) test.

2. Materials and methods

2.1. Data collection

Specimens were collected using several fishing techniques. Collection localities are given in Table 1. Collection and identification of *Champsocephalus esox* was provided by A. North (British Antarctic Survey), *Pagetopsis maculatus*, *Dacodraco hunteri*, *Cryodraco atkinsoni*, *Chionodraco myersi*, *Akarotaxis nudiceps*, and *Racovitzia glacialis* were collected by A.L. DeVries and identified by J.T. Eastman, *Neopagetopsis ionah*, *Chionobathyscus dewitti*, and *Chionodraco hamatus* were identified by T. Iwami. H.W. Detrich provided tissue for *Channichthys rhinoceratus*, *Bathydraco marri* and *Gerlachea australis* were collected and identified by C. Zimmermann. All other specimens were collected and identified by the senior author and deposited in the University of Tennessee Fish Collection (catalogue numbers available on request). Several species of the notothenioid family Bathydraconidae were selected as outgroup taxa for all phylogenetic analyses (Table 1). Muscle, spleen, or liver tissues were dissected from specimens and frozen in liquid nitrogen, or preserved in 95% ethanol. Nucleic acids were isolated from tissues using standard phenol–chloroform extraction and ethanol precipitation methods. The complete coding region of the mitochondrial NADH 2 (ND2) gene was amplified using primers GLN and ASN (Kocher et al., 1995), and the entire mitochondrially encoded large ribosomal subunit (16S) was amplified using newly developed primers Val-New (AGC ATC TCC CTT ACA CTG AGA AGT) and Leu-New (GTT AAG GAG AGG ACT TGA ACC TCT). PCR conditions are given in Near et al. (2000). PCR products were prepared for sequencing by digesting with 1.0 unit of Exonuclease I and shrimp alkaline phosphatase, and incubated for 15 min at 37 °C and 20 min at 80 °C. Treated PCR products were used as templates for Big Dye (Applied Biosystems) terminator cycle sequencing reactions. Four and six primers were used to sequence both strands of the ND2 and 16S genes respectively (primer sequences available upon request). Sequences were read with an ABI 377 automated sequencer at the W.M. Keck Center for Comparative and Functional Genomics at the University of Illinois Urbana–Champaign and the Division of Biological Sciences Automated DNA Sequencing Facility at the University of California, Davis. Complete gene sequences were assembled from individual sequencing reactions using the program Sequencher version 3.1 (Gene Codes, Ann Arbor, MI).

Morphological datasets published in Iwami (1985), Balushkin (2000), and Voskoboinikova (2000) were examined and all unique morphological characters were entered into MacClade 4.0 (Maddison and Maddison,

Table 1
Species sampled, collection localities, and GenBank accession numbers

Species	Family	Locality (latitude, longitude)
Champsocephalus esox	Channichthyidae	Falkland Islands (51°25′.0S, 57°35.0′W)
Champsocephalus gunnari	Channichthyidae	Palmer Archipelago (64°51.0′S, 63°34.0′W)
Champsocephalus gunnari	Channichthyidae	Elephant Island (61°11.7′S, 54°44.0′W)
Pagetopsis macropterus	Channichthyidae	South Shetland Islands (62°10.4′S, 60°28.4′W)
Pagetopsis maculatus	Channichthyidae	Ross Sea (77°19.0′S, 165°41.0′E)
Neopagetopsis ionah	Channichthyidae	Enderby Land (66°27.9′S, 48°32.6′E)
Pseudochaenichthys georgianus	Channichthyidae	Palmer Archipelago (64°51.0′S, 63°34.0′W)
Pseudochaenichthys georgianus	Channichthyidae	Elephant Island (61°17.3′S, 55°42.7′W)
Dacodraco hunteri	Channichthyidae	Ross Sea (77°19.0′S, 165°41.0′E)
Dacodraco hunteri	Channichthyidae	Ross Sea (77°19.0′S, 165°41.0′E)
Channichthys rhinoceratus	Channichthyidae	Kerguelen Islands
Chaenocephalus aceratus	Channichthyidae	Palmer Archipelago (64°51.0′S, 63°34.0′W)
Chaenocephalus aceratus	Channichthyidae	Elephant Island (61°04.0′S, 54°33.6′W)
Chionobathyscus dewitti	Channichthyidae	Enderby Land (66°27.9′S, 48°32.6′E)
Cryodraco antarcticus	Channichthyidae	Elephant Island (60°58.1′S, 55°04.8′W)
Cryodraco atkinsoni	Channichthyidae	Ross Sea (75°30.0′S, 174°56.0′E)
Chaenodraco wilsoni	Channichthyidae	South Shetland Islands (61°44.2′S, 58°20.5′W)
Chaenodraco wilsoni	Channichthyidae	South Shetland Islands (62°10.4′S, 60°28.4′W)
Chionodraco myersi	Channichthyidae	Ross Sea (75°30.0′S, 174°56.0′E)
Chionodraco hamatus	Channichthyidae	Prydz Bay (67°08.8′S, 75°17.1′E)
Chionodraco rastrospinosus	Channichthyidae	Elephant Island (61°10.1′S, 54°33.5′W)
Akarotaxis nudiceps	Bathydraconidae	Ross Sea (75°02.0′S, 166°16.0′E)
Bathydraco marri	Bathydraconidae	Weddell Sea (75°16.0′S, 26°39.0′W)
Racovitzia glacialis	Bathydraconidae	Ross Sea (75°30.0′S, 174°56.0′E)
Gerlachea australis	Bathydraconidae	Weddell Sea (75°00.0′S, 28°00.0′W)
Gymnodraco acuticeps	Bathydraconidae	McMurdo Sound (75°51.0′S, 166°40.0′E)
Gymnodraco acuticeps	Bathydraconidae	Palmer Archipelago (64°51.0′S, 63°34.0′W)

2000). Character states for *Chionobathyscus dewitti* are scored as missing for the 15 unique characters from Voskoboinikova (2000), because character coding was not provided for this species. A total of 58 characters were assembled from these datasets, four characters were multistate, and 54 were binary characters (Table 2, Appendix A).

2.2. Data analysis

Complete gene sequences of ND2 were aligned by eye, as there were no insertions or deletions (indels) in the sequences. 16S rRNA sequences were aligned based on secondary structural elements and conserved motifs, by comparing to existing models of secondary structure for large subunit rRNAs (Gutell and Fox, 1988; Gutell et al., 1993; De Rijk et al., 2000). Structural designation of nucleotide positions were paired and unpaired. Unpaired bases included bulges, loops, and unpaired positions. The pooling of these classes of characters as unpaired positions was justified in finding no difference in rate of change or nucleotide composition among the three designated categories. These regions of the notothenioid 16S rRNA were initially identified by aligning the *Pagetopsis macropterus* 16S gene with the 16S rRNA secondary structure model for the cyprinid fish *Cyprinus carpio*.

The presence of multiple substitutions, or saturation in the ND2 and 16S sequences was investigated by plotting numbers of observed transitions versus transversions. These plots were constructed for each codon position in ND2 and for substitutions in paired and unpaired regions of the 16S rRNA. Variance of nucleotide composition in each of the designated character classes (i.e. codon positions, secondary structural elements) among taxa was estimated using a χ^2 heterogeneity test, both for all sites and variable sites only.

Phylogenetic trees were constructed with MP using the computer program PAUP* 4.0b10 (Swofford, 2000) for each of the mtDNA gene region partitions (ND2 and 16S) and the morphological data partition, as well as combined mtDNA gene regions and morphology. MP topologies were obtained using a heuristic tree search, with TBR branch swapping, and 100 addition sequence replicates. Qualitative support for recovered nodes was assessed using a non-parametric bootstrap analysis with 2000 pseudoreplicates. We assessed the degree of phylogenetic incongruence between the three data partitions (ND2, 16S, and morphology), using the MP incongruence-length difference (ILD) method (Farris et al., 1994), as implemented by the partition-homogeneity test in PAUP*, with 1000 replications using a heuristic tree search with 5 addition sequence replicates. Each combination of data partitions was considered.

Table 2
Character state matrix for morphological characters

Species	1	2	3	4	5	6	7	8	9	10	11	12	13	14	15
Bathydraconidae	0	0	0	0	0	0	0	0	0	0	0	0	0	0	0
Chaenocephalus aceratus	1	1	1	1	1	1	1	1	1	1	1	0	0	0	0
Cryodraco antarcticus	1	1	1	1	1	1	1	1	1	1	1	0	0	0	0
Cryodraco atkinsoni	1	1	1	1	1	1	1	1	1	1	1	0	0	0	0
Chionobathyscus dewitti	1	1	1	1	1	1	1	1	1	1	1	0	0	0	0
Champsocephalus esox	1	1	0	0	0	0	0	0	0	1	1	0	0	1	0
Champsocephalus gunnari	1	1	0	0	0	0	0	0	0	1	1	0	0	1	0
Chionodraco hamatus	1	1	1	1	1	1	1	1	1	1	1	0	0	0	0
Chionodraco myersi	1	1	1	1	1	1	1	1	1	1	1	0	0	0	0
Chionodraco rastrospinosus	1	1	1	1	1	1	1	1	1	1	1	0	0	0	0
Channichthys rhinoceratus	0	0	0	0	0	1	0	0	1	1	1	0	0	0	0
Chaenodraco wilsoni	1	1	1	1	1	1	1	1	1	1	1	0	0	0	0
Dacodraco hunteri	1	1	1	1	1	1	1	1	1	0	1	0	0	0	1
Neopagetopsis ionah	1	1	1	1	1	1	0	0	0	0	1	1	1	1	1
Pseudochaenichthys georgianus	1	1	1	1	1	1	0	0	0	0	0	1	1	1	1
Pagetopsis macropterus	1	1	1	1	1	1	0	0	0	0	0	1	1	1	1
Pagetopsis maculatus	1	1	1	1	1	1	0	0	0	0	0	1	1	1	1

Species	16	17	18	19	20	21	22	23	24	25	26	27	28	29	30
Bathydraconidae	0	0	0	0	0	0	0	0	0	0	0	0	0	0	0
Chaenocephalus aceratus	1	1	1	0	0	0	1	1	0	0	0	0	1	0	0
Cryodraco antarcticus	1	1	1	0	1	1	1	1	0	1	0	0	1	0	1
Cryodraco atkinsoni	1	1	1	0	1	1	1	1	0	1	0	0	1	0	1
Chionobathyscus dewitti	0	0	0	1	1	1	0	1	0	1	0	0	1	1	0
Champsocephalus esox	0	0	0	0	0	0	0	0	0	1	0	0	1	0	0
Champsocephalus gunnari	0	0	0	0	0	0	0	0	0	1	0	0	1	0	0
Chionodraco hamatus	0	0	0	1	1	1	0	0	0	1	1	1	1	0	1
Chionodraco myersi	0	0	0	1	1	1	0	0	0	1	1	1	1	0	1
Chionodraco rastrospinosus	0	0	0	1	1	1	0	0	0	1	1	1	1	0	1
Channichthys rhinoceratus	0	1	1	0	0	0	0	0	0	0	0	1	1	0	0
Chaenodraco wilsoni	0	0	0	1	1	1	0	1	0	1	1	1	1	0	0
Dacodraco hunteri	1	1	1	0	1	0	0	0	0	1	0	0	1	0	0
Neopagetopsis ionah	0	0	1	0	1	1	0	0	1	0	0	0	0	1	0
Pseudochaenichthys georgianus	0	0	0	0	1	0	0	0	0	0	0	0	0	0	1
Pagetopsis macropterus	0	0	1	0	0	0	0	0	1	0	0	1	0	0	1
Pagetopsis maculatus	0	0	1	0	0	0	0	0	1	0	0	1	0	0	1

Species	31	32	33	34	35	36	37	38	39	40	41	42	43	44	45
Bathydraconidae	0	0	0	0	0	0	0	0	0	0	0	0	0	0	0
Chaenocephalus aceratus	1	0	0	1	0	1	0	0	1	1	1	0	0	2	3
Cryodraco antarcticus	1	1	0	1	0	0	0	0	1	1	1	0	0	1	2
Cryodraco atkinsoni	1	1	0	1	0	0	0	0	1	1	1	0	0	1	2
Chionobathyscus dewitti	1	1	0	1	0	0	0	0	1	1	1	0	0	?	?
Champsocephalus esox	1	0	0	0	0	0	1	0	0	0	0	0	0	0	0
Champsocephalus gunnari	1	0	0	0	0	0	1	0	0	0	0	0	0	0	0
Chionodraco hamatus	1	1	1	1	0	0	0	0	1	1	1	0	0	1	0
Chionodraco myersi	1	1	1	1	0	0	0	0	1	1	1	0	0	1	0
Chionodraco rastrospinosus	1	1	1	1	0	0	0	0	1	1	1	0	0	1	0
Channichthys rhinoceratus	0	0	0	1	1	0	0	1	1	1	1	1	0	1	2
Chaenodraco wilsoni	0	0	0	1	0	0	0	0	1	1	1	0	1	0	0
Dacodraco hunteri	0	1	0	1	0	0	0	0	1	1	1	0	0	2	1
Neopagetopsis ionah	0	0	0	1	0	0	0	0	0	0	0	0	0	2	2
Pseudochaenichthys georgianus	0	0	1	1	0	0	0	0	0	0	0	0	0	2	2
Pagetopsis macropterus	0	0	0	1	0	0	0	0	0	0	0	0	0	1	2
Pagetopsis maculatus	0	0	0	1	0	0	0	0	0	0	0	0	0	1	2

Species	46	47	48	49	50	51	52	53	54	55	56	57	58
Bathydraconidae	0	0	1	1	0	0	0	0	1	0	0	0	0
Chaenocephalus aceratus	0	2	1	1	0	0	1	1	1	1	0	1	0
Cryodraco antarcticus	0	2	1	1	0	0	1	1	1	1	0	1	0
Cryodraco atkinsoni	0	2	1	1	0	0	1	1	1	1	0	1	0

Table 2 (*continued*)

Species	1	2	3	4	5	6	7	8	9	10	11	12	13	14	15
Chionobathyscus dewitti	?	?	?	?	?	?	?	?	?	?	?	?	?		
Champsocephalus esox	0	0	1	1	0	0	0	0	1	0	0	1	0		
Champsocephalus gunnari	0	0	1	1	0	0	0	0	1	0	0	1	0		
Chionodraco hamatus	0	2	1	1	0	0	0	1	1	1	1	1	0		
Chionodraco myersi	0	2	1	1	0	0	0	1	1	1	1	1	0		
Chionodraco rastrospinosus	0	2	1	1	0	0	0	1	1	1	1	1	0		
Channichthys rhinoceratus	0	2	1	1	1	0	1	0	1	1	0	0	0		
Chaenodraco wilsoni	0	2	1	1	0	0	1	1	1	1	0	1	0		
Dacodraco hunteri	1	1	0	0	0	1	0	0	0	0	1	0	1		
Neopagetopsis ionah	2	2	1	1	0	0	1	1	1	0	0	1	0		
Pseudochaenichthys georgianus	3	3	1	1	0	0	1	1	1	1	0	0	0		
Pagetopsis macropterus	2	2	1	1	0	0	1	1	1	0	0	0	0		
Pagetopsis maculatus	2	2	1	1	0	0	1	1	1	0	0	0	0		

See Appendix A for character and character state descriptions.

2.3. Comparison of alternative tree topologies

Alternative phylogenetic hypotheses (Fig. 1) were compared to tree topologies generated from analysis of the combined mtDNA and morphology dataset. MP heuristic tree searches with topological constraints were used to find the most-parsimonious trees that were consistent with previous hypotheses of channichthyid relationships (Fig. 1). The alternative phylogenetic hypotheses considered were the morphological-inferred trees from Iwami (1985), Balushkin (2000), and Voskoboinikova (2000), and the mtDNA-inferred tree from Chen et al. (1998).

The significance of tree length differences between trees recovered in MP analyses and alternative tree topologies has typically been assessed using a parsimony modified Kishino–Hasegawa test (Kishino and Hasegawa, 1989). As pointed out by Goldman et al. (2000), this test assumes no tree length differences between competing topologies as the null hypothesis. Since the tree recovered in MP analysis will by definition be the shortest tree, the condition of the null hypotheses is violated by comparing a tree resulting from analysis of the dataset to alternative topologies. The appropriate test is one with a null hypothesis stating that all trees considered are equally good explanations of the data (Goldman et al., 2000; Shimodaira and Hasegawa, 1999). The test most appropriate for this null hypothesis is the Shimodaira-Hasegawa (SH) test and has been designed for use in maximum likelihood (ML) optimality criteria. We are prevented from searching for the best trees that represent the alternative hypotheses using the combination of mtDNA and morphological data partitions using ML, because ML methods for dealing with mixed models in combined molecular and morphological data partitions are not readily available (Lewis, 2001). Therefore, we have modified the SH test to compare the tree length differences from the MP inferred tree, and the four alternative hypotheses of channichthyid relationships using MP optimality criteria (Fig. 1).

We calculated the tree length difference (δ_χ) between the tree resulting from MP analysis (T_{MP}) and each alternative tree topology (T_χ), such that $\delta_\chi = T_{MP} - T_\chi$. The significance of δ_χ for topology T_χ was determined by constructing a bootstrap distribution of δ_χ (Goldman et al., 2000; Shimodaira and Hasegawa, 1999). One hundred nonparametric bootstrap datasets were generated using Seqboot in Phylip (Felsenstein, 1993), and the tree length for each alternative tree at each replicate i was calculated, and designated as $T_{\chi BS}^{(i)}$. For each $T_{\chi BS}^{(i)}$, the difference between $T_{\chi BS}^{(i)}$ and the mean tree length across all bootstrap replicates was calculated, giving $\sim T_{\chi BS}^{(i)}$. This is the centering procedure that enforces the resampled data to conform to the null hypothesis for this a posteriori test (Goldman et al., 2000). For each replicate i, the MP tree length was determined and designated as $T_{MP}^{(i)}$. For each replicate the $T_{MP}^{(i)}$ value was centered by calculating the difference between $T_{\chi MP}^{(i)}$ and the mean tree length across all bootstrap replicates, giving $\sim T_{\chi MP}^{(i)}$. The bootstrap replicate statistic $\delta^{(i)}$ was formed by determining $\sim T_{MP}^{(i)} - \sim T_{\chi BS}^{(i)}$ for each replicate i. For each alternative topology T_χ, the significance of δ_χ was determined by comparing to the distribution of $\delta_\chi^{(i)}$ over i replicates, by 0 and 95% of the ranked list of $\delta_\chi^{(i)}$. The test is one-tailed, and a 5% significance level was used.

3. Results

The complete ND2 and 16S rRNA genes were sequenced for all specimens sampled (Table 1). Sequences were submitted to GenBank with Accession Nos. AY249459–AY249512. The protein coding ND2 gene was the 1047 base pairs (bp), and the translated proteins are 348 amino acids long with no indels in all species sampled. Within the Channichthyidae, the 16S rRNA ranged in size from 1690 to 1693 bp. The aligned length of the 16S rRNA sequences, including five bathydraconid species was 1703 bp. Table 3 summarizes the size of each mtDNA gene region, numbers of variable and

Table 3
Summary of variation among each gene and structural categories or character classes within the Channichthyidae

Gene	Structural category or character class	No. of aligned sites (% of all)	No. of variable sites (% of aligned sites in class)	No. of informative sites (% of aligned sites in class)
16S	Paired	658 (38.6)	23 (3.5)	16 (2.4)
	Unpaired	1045 (61.4)	104 (10.0)	78 (7.5)
	All	1703 (100.0)	127 (7.5)	94 (5.5)
ND2	First codon	349 (33.3)	33 (9.5)	21 (6.0)
	Second codon	349 (33.3)	15 (4.3)	9 (2.6)
	Third codon	349 (33.3)	183 (52.4)	148 (42.4)
	All	1047 (100.0)	231 (22.1)	178 (17.0)

phylogenetically informative sites, categorized by structural category and character class. The percentage of variable sites in 16S rRNA is much lower than in ND2, reflecting the observation that in the mtDNA genome, protein coding genes exhibit a higher rate of nucleotide substitution than rRNA genes (Meyer, 1993; Pesole et al., 1999).

ND2 sequences in the sampled notothenioid species exhibit marked deviation from equal frequency when all sites and each codon position are considered. The compositional bias exhibited in ND2 is very similar values reported for East African cichlids (Kocher et al., 1995), and reflects typical a lack of guanine in vertebrate mtDNA protein coding genes (Meyer, 1993). The nucleotide biases in the entire 16S rRNA is expressed as an over-representation of adenine and an under-representation of guanine and thymine, or uracil. Compositional biases in channichthyid 16S rRNA genes differ between paired and unpaired regions. Unpaired regions exhibit a marked over-representation of adenine and are lacking guanine. Paired regions are biased with an over-representation of guanine and cytosine, and a lack of adenine and thymine. These patterns are similar to those reported for partial 16S sequences in characiform fishes (Orti et al., 1996). The biases exhibited in 16S rRNA are hypothesized to be related to the structure and function of the molecule. The richness of adenine in unpaired regions may be due to fact that adenine is the least polar of the nucleotides, facilitating hydrophobic interactions of the unpaired regions with ribosomal proteins (Vawter and Brown, 1993). The greater occurrence of guanine and cytosine in the paired regions of 16S is explained by the lower free energy of the G–C bonds, relative to A–T or G–T bonds (Vawter and Brown, 1993). There was no significant differences among species in nucleotide composition in all sites and variable sites in each of the two mitochondrial genes and all structural categories and character classes presented in Table 3 (all χ^2 tests $P > 0.9$).

Bias in nucleotide variation by codon position in the ND2 gene is evident (Table 3), and this pattern has been reported from other phylogenetic analyses of closely related actinopterygian lineages using ND2 sequences (Breden et al., 1999; Broughton and Gold, 2000; Kocher et al., 1995). The third codon position is the most variable followed by the first and second codon positions. The greatest percentage of phylogenetically informative sites contributed by any structural category among ND2 and 16S is the ND2 third codon position. As previously reported for actinopterygian mtDNA rRNA genes (Orti et al., 1996), the unpaired regions of the 16S have a higher percentage of variable and phylogenetically informative sites than the paired regions (Table 3).

Plotting absolute numbers of transitions versus transversions indicate that third codon positions may be approaching marginal saturation in comparisons between Bathydraconidae and Channichthyidae. Within channichthyids, changes in first and third codon positions do not appear to reach a plateau in the plot, indicating that these sites are not saturated with multiple substitutions. Saturation plot of 16S does not reveal any noticeable pattern of multiple substitutions. This result parallels a similar finding from examination of partial 12S and 16S rRNA gene sequences sampled from a greater diversity of notothenioid lineages (Ritchie et al., 1997).

MP analyses of all datasets are summarized in Table 4. The Channichthyidae was monophyletic in all analyses (Figs. 2 and 3). Phylogenetic topologies from ND2 and 16S rRNA are congruent, but ND2 provides greater resolution (100% of nodes recovered versus 46.7%) throughout the channichthyid phylogeny (Table 4). Combining the ND2 and 16S rRNA genes results in complete resolution with a much greater percentage of nodes supported with 70% or greater bootstrap pseudoreplicate scores than either mtDNA gene region alone (Fig. 2, Table 4). The morphology dataset provides better phylogenetic resolution than the 16S rRNA, and the proportion of nodes with bootstrap support is higher than in the ND2 analysis (Fig. 2, Table 4). The greatest phylogenetic resolution, in terms of percentage of nodes supported in bootstrap analysis was the combined mtDNA and morphology data partitions, with nearly 90% of all possible nodes supported (Fig. 3, Table 4).

Examination of phylogenetic incongruence among the datasets, as measured by the ILD test is presented

Table 4
Summary of maximum parsimony analyses

Dataset	No. of trees recovered	Tree length (CI[a])	Percent nodes recovered[b]	Percent nodes bootstrap $\geqslant 70\%$[b]
ND2	1	751 (0.570)	100.0	46.7
16S	11	381 (0.580)	46.7	26.7
mtDNA[c] (Fig. 2)	1	1136 (0.571)	100.0	73.3
Morphology (Fig. 2)	4	112 (0.565)	80.0	60.0
All data combined[d] (Fig. 3)	1	1256 (0.565)	100.0	86.7

[a] Consistency index, excluding phylogenetically uninformative characters.

[b] Percentage of all possible nodes, a fully resolved tree will have $n - 1$ nodes, where n, number of taxa in analysis.

[c] Combined ND2 and 16S.

[d] Combined mtDNA and morphology.
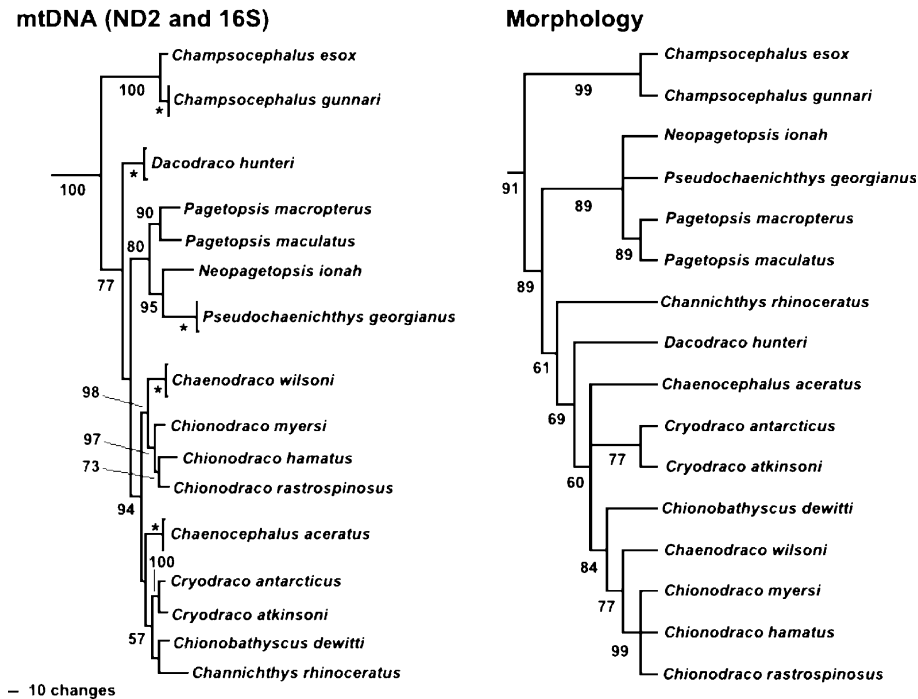
Fig. 2. Single tree resulting from maximum parsimony analysis of the combined ND2 and 16S data partitions (left). Tree is drawn as a phylogram, where the length of a given branch is scaled to the amount of character change. All intraspecific nodes were recovered in 100% of the bootstrap pseudoreplicates, and are indicated with an asterisk. Strict consensus of four trees resulting from maximum parsimony analysis of 58 morphological characters (right). Only the portion of the tree containing the channichthyids is shown. Percent recovery of bootstrap pseudoreplicates are indicated at the node. See Table 4 for tree statistics.

in Table 5. The lowest incongruence was observed between the two mtDNA gene partitions. Comparisons between the individual mtDNA data partitions and morphology did not result in a significant *P* value. However, the ILD test of mtDNA (combined ND2 and 16S) versus morphology resulted in a marginally significant *P* value (Table 5). The tree topologies resulting from the combined mtDNA partitions and the morphological data set (Fig. 2) are congruent except for the placement of *Channichthys rhinoceratus*. The mtDNA gene tree (Fig. 2) indicates that *Channichthys rhinoceratus* is derived in the channichthyid tree, placed apical as the sister species of *Chionobathyscus dewitti*. In contrast, the morphology inferred tree (Fig. 2) places

Channichthys rhinoceratus in a relatively basal position as the sister taxon of a large clade containing the genera *Dacodraco*, *Chaenocephalus*, *Cryodraco*, *Chionobathyscus*, *Chaenodraco*, and *Chionodraco*. The difference in the placement of *Channichthys rhinoceratus* in the mtDNA and morphology data partition analyses may be the reason that there is a significant, though marginal, result in the ILD test when comparing these two data partitions (Table 5).

When compared to the tree resulting from the MP analysis of the combined mtDNA and morphology data partitions (Fig. 3), two of the four previous hypotheses of relationships of channichthyids (Fig. 1) were significantly different in the parsimony-based SH test
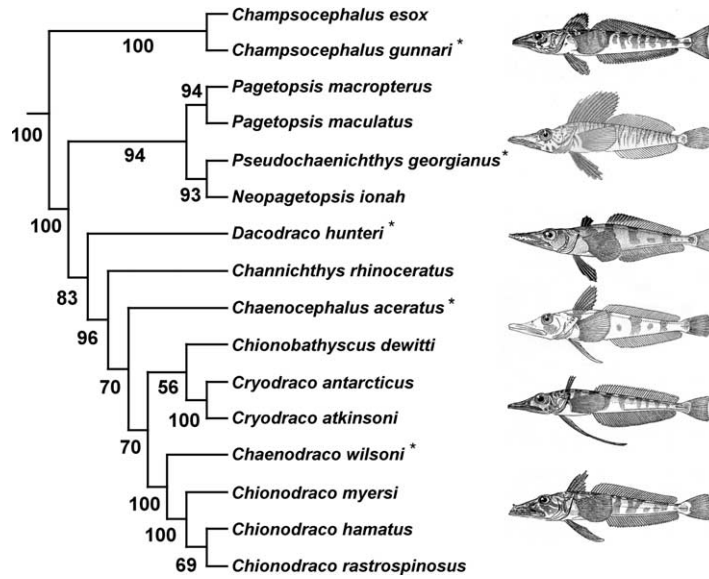
Fig. 3. Single tree resulting from maximum parsimony analysis of the combined ND2, 16S, and morphology data partitions. Percent recovery of bootstrap pseudoreplicates are indicated at the node. Representative channichthyid species illustrated on the right [modfied from Andriashev (1965) and Norman (1938)]. An asterisk indicates species that were sampled with two individuals (intraspecific nodes not shown).

Table 5
Results of ILD tests between datasets for Channichthyidae

Datasets compared	P value
ND2 vs. 16S	0.919
ND2 vs. morphology	0.116
16S vs. morphology	0.143
mtDNA vs. morphology	0.045*
ND2 vs. 16S vs. morphology	0.260

Asterisked values indicate significant differences at $P < 0.05$.

Fig. 4. Distribution of tree length differences in 100 nonparametric bootstrap replicates in the Shimodaira–Hasegawa test. Observed tree length differences (δ) between the maximum parsimony tree (Fig. 3) and four alternative hypotheses (Fig. 1) are shown on the distribution. $\delta_1 =$ Chen et al. (1998), $\delta_2 =$ Iwami (1985), $\delta_3 =$ Voskoboinikova (2000), and $\delta_4 =$ Balushkin (2000).

(Table 6). The distribution of tree length differences between the combined data partition MP tree and each alternative hypothesis among 100 bootstrap replicates is presented is shown in Fig. 4. This distribution permits assessment of the significance of alternative hypotheses of channichthyid relationships. The hypotheses presented by Chen et al. (1998) and Iwami (1985) are five and six steps longer than the MP tree respectively (Fig. 4, Table 6), and are not significantly different from the combined data partition MP tree (Fig. 3). The tree topologies proposed by Voskoboinikova (2000) and Balushkin (2000), are each longer than 95% of all bootstrap replicated tree length differences (Fig. 4), and

Table 6
Comparison of alternative tree topologies[a] Using maximum parsimony Shimodaira–Hasegawa tests of the combined molecular and morphology dataset

Tree	No. of trees recovered	Tree length (CI[b])	Tree length difference ($\delta\chi$)	P value
Combined partitions (Fig. 3)	1	1256 (0.565)	Best	–
Chen et al. (1998)	1	1261 (0.563)	5	>0.328
Iwami (1985)	1	1262 (0.563)	6	>0.278
Voskoboinikova (2000)	1	1279 (0.555)	23	<0.020*
Balushkin (2000)	1	1308 (0.541)	52	<0.001*

Asterisked values indicate significant differences at $P < 0.05$. See Fig. 4 for test distribution of nonparametric SH test.
[a] See Fig. 1.
[b] Consistency index, excluding phylogenetically uninformative characters.

hence are significantly different from the combined data partition MP tree (Table 6).

4. Discussion

Previous hypotheses of relationships in the Channichthyidae have been based on analyses of different datasets, and no two analyses have resulted in a completely congruent tree topology (Fig. 1). Interestingly, among the three published morphological datasets used to investigate phylogenetic relationships of channichthyids, all differ in the composition of characters, and no study subsequent to Iwami (1985) has included all published morphological characters in a single phylogenetic analysis. Similarly previous mtDNA sequence analysis of channichthyid phylogeny did not examine congruence of molecular and morphological data with ILD tests, or phylogenetic analyses of combined data partitions. The results of this study using the complete nucleotide sequences of two mtDNA genes and all available morphological characters, demonstrate that there is marginal to insignificant phylogenetic incongruence among the data partitions, and the greatest phylogenetic resolution is achieved when these characters are combined into a single analysis (Fig. 3). Also, combining data partitions provides exceptional potential to discriminate among alternative phylogenetic hypotheses (Fig. 4, Table 6).

If the tree topology resulting from MP analysis of the combined mtDNA and morphology data partitions is accepted as the phylogenetic hypotheses that best encompasses all of the available data, then an examination of the similarities and differences between this tree (Fig. 3) and previous hypotheses (Fig. 1) is warranted. First, the combined data MP tree is very similar to most previous hypotheses, especially with regard to the monophyly of two clades, *Pagetopsis–Pseudochaenichthys–Neopagetopsis*, and *Chaenodraco–Chionodraco*. The combined data partitions MP tree (Fig. 3) and all previous hypotheses, except Balushkin (2000) recover *Champsocephalus* as the sister taxon to all other channichthyids. The substantial MP tree length difference between the combined data MP tree and the tree proposed by Balushkin (2000) is probably a result of placing *Channichthys rhinoceratus*, instead of *Champsocephalus*, as the sister taxon to all other channichthyids (Table 6). The combined data partitions MP tree is congruent with Chen et al. (1998) and Voskoboinikova (2000) with respect to the phylogenetic placement of *Dacodraco* (Figs. 1 and 3). All of these hypotheses place *Dacodraco* as the sister taxon to a monophyletic clade containing *Channichthys*, *Chaenocephalus*, *Chionobathyscus*, *Cryodraco*, *Chaenodraco*, and *Chionodraco*. The combined data MP tree (Fig. 3) and the topologies proposed by Iwami (1985) and Chen et al. (1998) recover *Cryodraco* and *Chionobathyscus* as sister taxa.

The most novel contribution of the combined data MP analysis is the strong resolution in the phylogenetic placement of *Channichthys rhinoceratus* and *Chaenocephalus aceratus*. All previous hypotheses disagree on the phylogeny of these two species (Fig. 1). The combined data partitions MP tree places *Channichthys rhinoceratus* and *Chaenocephalus aceratus* as sequential sister species to a clade containing mostly wide-distributed circum-Antarctic species (Fig. 3). The nodes connecting these species to their respective sister taxa are well-supported in bootstrap analysis (Fig. 3), a result not in conflict with separate analyses of mtDNA and morphology, since neither dataset offered strong resolution in the placement of these species (Fig. 2). This result is interesting because *Channichthys rhinoceratus* is endemic to the Kerguelen-Heard Islands, and *Chaenocephalus aceratus* is endemic to the Antarctic Peninsula, South Orkney Islands, South Georgia, South Sandwich Islands, and Bouvet Island (Iwami and Kock, 1990). It is possible that the wide distribution of species in the portion of the channichthyid tree that contains *Chionobathyscus*, *Cryodraco*, *Chaenodraco*, and *Chionodraco* represents recent range expansions subsequent to speciation. The ancestral area for these species of channichthyids may comprise the peri-Antarctic regions occupied by *Channichthys rhinoceratus* and *Channichthys aceratus*.

The Notothenioidei represents an understudied and evolutionarily rich adaptive radiation in the coastal waters of Antarctica. The Channichthyidae are only one exemplar clade in this exceptional radiation of fishes. Morphological and ecological diversity among the channichthyids is substantial; however, testing hypotheses of diversification and adaptive radiation in this clade has been hampered by a lack of understanding phylogenetic relationships, and appreciable incongruence among existing phylogenetic hypotheses. In this study we have presented a robust phylogenetic hypothesis for the Channichthyidae that utilizes all available discretely coded morphological data, and a substantial mtDNA sequence dataset. This phylogeny should serve as the basis for investigating the geographic components of speciation, rates of diversification, and the origin of ecological and morphological diversity in this unique clade of fishes.

Appendix A

Character and character state descriptions. The source of the character is given in parentheses; I, Iwami (1985); B, Balushkin (2000); and V, Voskoboinikova (2000). The number following corresponds to character number from the source.

1. Scapular foramen (B1, V22); 0: only in scapula, 1: between scapula and coracoid. **2**. Tubular lateral line scales (B2); 0: ossified, 1: weakly ossified. **3**. Pelvic fin (B3, I15, V25); 0: normal shape, 1: elongated, fan-like, or cane-like. **4**. Pterosphenoid (B4, I2, V6); 0: borders sphenoid; 1: separated from sphenoid by band of cartilage. **5**. Anterior branch of median lateral line (B5); 0: well-developed, no. of scales more than 20; 1: reduced, no. of scales no more than 20. **6**. Ectopterygoid-quadrate (B6, I8); 0: bordered, or overlapping; 1: separate. **7**. Pelvic fin (B7, V23); 0: third ray longest; 1: second ray longest. **8**. Number of caudal vertebrae (B8); 0: 15–21; 1: 22–34. **9**. Third hypobranchial (B9, I13, V21); 0: flat and triangular; 1: elongate and cane-like. **10**. Posterior subopercle (B10, V15); 0: ossified; 1: not ossified. **11**. Dorsal lateral line (B11); 0: less than 85 tubular scales; 1: more than 90 tubular scales. **12**. Ventral expansion on second infraorbital (B12, I5); 0: absent; 1: present. **13**. Pelvic fin (B13); 0: without broad membranes; 1: fan-shaped with broad membranes. **14**. Branchiostegal radii on ceratohyal (B14); 0: four; 1: five or more. **15**. Outer margin of sub- and interopercle (B15); 0: thickened; 1: not thickened. **16**. Dorsal fins (B16); 0: not separated; 1: well separated. **17**. Neurocranium width relative to snout (B17); 0: less extended snout; 1: narrow with elongated snout. **18**. Gill rakers (B18); 0: with spines; 1: reduced, if present without spines. **19**. Second dorsal fin (B19); 0: origin of fin more than 1/5 of vertebral column from head; 1: origin of fin less than 1/5 of vertebral column from head. **20**. Anal lateral line (B20, V31); 0: absent; 1: present. **21**. Anal lateral line (B21); 0: usually less than 60 tubular scales; 1: usually more than 60 tubular scales. **22**. Pelvic fin rays (B22, V24); 0: not elongated; 1: elongated, reach further than tenth ray of anal fin. **23**. Tubular scales in dorsal lateral line (B23); 0: less than 112; 1: 112–135. **24**. First dorsal fin; 0: not enlarged; 1: enlarged, sail-like shape. **25**. Posterior margin of orbit (B25); 0: crenulated; 1: smooth. **26**. Spines on sub- and interopercle (B26, I10, V16); 0: absent; 1: present. **27**. Cavity in radial 3 (B27); 0: absent; 1: present. **28**. Caudal fin rays, modal number (B28, I17, V27); 0: 12; 1: 11. **29**. Postcoracoid process (B29); 0: elongated; 1: short. **30**. Temporal canal, first pore (B30); 0: present; 1: absent. **31**. rostral spine (B31); 0: present; 1: reduced. **32**. First dorsal fin spines (B32); 0: more than 5; 1: usually not more than 5. **33**. Preopercle-mandibular canal, temporal canal (B33); 0: not connected; 1: connected. **34**. Origin of supraorbital canal (I1); 0: anterior region; 1: orbital region. **35**. Tubercles on dermal bones (I3); 0: absent; 1: present. **36**. Dorsal expansion on first infraorbital (I4); 0: absent; 1: present. **37**. Number of infraorbital bones (I6, V9); 0: 6 or 7; 1: 8 or 9. **38**. Bony plate on lateral line (I7, V29); 0: absent; 1: present. **39**. Opercle spine (I9); 0: unbranched; 1: well branched. **40**. Branchiostegal rays (I11, V20); 0: 7 or more; 1: 6. **41**. Dorsal hypohyal (I12, V19); 0: ossified; 1: not ossified. **42**. Coracoid notch (I14); 0: absent; 1: present. **43**. Pelvic fin soft rays (I16, V26); 0: five; 1: four. **44**. Ratio of ethmoid length to neurocranium minus ethmoid (V1); 0: less than 60%; 1: less than 90%; 2: greater than 90%. **45**. Width of ethmoid division at level of mesethmoid (V2); 0: 20–30%; 1: 10–20%; 2: 30–40%; 3: 40–50%. **46**. Width of ethmoid division (V3); 0: 60–70%; 1: 40–50%; 2: 70–80%; 3: 80–90%. **47**. Direction of anterior branch of parasphenoid (V4); 0: upward; 1: horizontal; 2: downward. **48**. Openings on prootic (V5); 0: two; 1: one. **49**. Prominent groove on prootic and exoccipital (V7); 0: present; 1: absent. **50**. Integumentary bones of skull (V8); 0: smooth; 1: with expressed sculpture. **51**. Posterior of lachrimal with expressed lengthening and thickening (V11); 0: absent; 1: present. **52**. Opening between quadrate, symplectic, and preopercle (V12); 0: large and triangular; 1: small and narrow. **53**. Vertical and horizontal branch of preopercle (V13); 0: equal or nearly equal to 90 degrees; 1: angle obtuse. **54**. Vertical branch of preopercle (V14); 0: not widened upward; 1: widened upward. **55**. Bony membrane between vertical and horizontal branch of operculum (V17); 0: well-developed; 1: poorly developed; 2: completely reduced, replaced with spines. **56**. Teeth on jaws (V18); 0: undifferentiated; 1: differentiated, small and pointed. **57**. Modal number of vertebrae (V28); 0: less than 57; 1: greater or equal to 57. **58**. Median lateral line (V30); 0: tubular non-perforated scales; 1: small perforated scales.

References

Andriashev, A.P., 1965. A general review of the Antarctic fish fauna. In: Mieghem, J.v., Oye, P.v. (Eds.), Biogeography and Ecology in Antarctica. The Hague, Junk, pp. 491–550.

Balushkin, A.V., 2000. Morphology, classification, and evolution of notothenioid fishes of the Southern Ocean (Notothenioidei, Perciformes). J. Ichthyol. 40, S74–S109.

Bargelloni, L., Marcato, S., Zane, L., Patarnello, T., 2000. Mitochondrial phylogeny of notothenioids: a molecular approach to Antarctic fish evolution and biogeography. Syst. Biol. 49, 114–129.

Breden, F., Ptacek, M.B., Rashed, M., Taphorn, D., Figueiredo, C.A., 1999. Molecular phylogeny of the live-bearing fish genus *Poecilia* (Cyprinodontiformes: Poeciliidae). Mol. Phylogenet. Evol. 12, 95–104.

Broughton, R.E., Gold, J.R., 2000. Phylogenetic relationships in the North American cyprinid genus *Cyprinella* (Actinopterygii: Cyprinidae) based on sequences of the mitochondrial ND2 and ND4L genes. Copeia 2000, 1–10.

Chen, W.-J., Bonillo, C., Lecointre, G., 1998. Phylogeny of the Channichthyidae (Notothenioidei, Teleostei) based on two mitochondrial genes. In: di Prisco, G., Pisano, E., Clarke, A. (Eds.), Fishes of Antarctica: A Biological Overview. Springer, Berlin, pp. 287–298.

Clarke, A., Johnston, I.A., 1996. Evolution and adaptive radiation of Antarctic fishes. Trends Ecol. Evol. 11, 212–218.

De Rijk, P., Wuyts, J., Peer, Y.V.d., Winkelmans, T., Wachter, R.D., 2000. The European large subunit ribosomal RNA database. Nucleic Acids Res. 28, 177–178.

Eakin, R.R., 1981. Osteology and relationships of the fishes of the Antarctic family Harpagiferidae (Pisces, Notothenioidei). In: Kornicker, L.S. (Ed.), Antarcic Research Series, vol. 31, Biology of the Antarctic Seas IX. American Geophysical Union, Washington, pp. 81–147.

Eastman, J.T., 1993. Antarctic Fish Biology: Evolution in a Unique Environment. Academic Press, San Diego.

Eastman, J.T., Eakin, R.R., 2000. An updated species list of notothenioid fish (Perciformes; Notothenioidei), with comments on Antarctic species. Arch. Fish. Mar. Res. 48, 11–20.

Farris, J.S., Kallersjo, M., Kluge, A.G., Bult, C., 1994. Testing significance of incongruence. Cladistics 10, 315–319.

Felsenstein, J., 1993. PHYLIP: Phylogenetic Inference Package, 3.5c ed University of Washington, Seattle.

Goldman, N., Anderson, J.P., Rodrigo, A.G., 2000. Likelihood-based tests of topologies in phylogenetics. Syst. Biol. 49, 652–670.

Gutell, R.R., Fox, G.E., 1988. A compilation of large subunit RNA sequences presented in structural format. Nucleic Acids Res. 16r, r175–r225.

Gutell, R.R., Gray, M.W., Schnare, M.N., 1993. A compilation of large subunit (23S and 23S-like) ribosomal RNA structures: 1993. Nucleic Acids Res. 21, 3055–3074.

Hemmingsen, E.A., 1991. Respiratory and cardiovascular adaptations in hemoglobin-free fish: resolved and unresolved problems. In: di Prisco, G., Maresca, B., Tota, B. (Eds.), Biology of Antarctic Fish. Springer, Berlin, pp. 191–203.

Iwami, T., 1985. Osteology and relationships of the family Channichthyidae. Mem. Nat. Inst. Polar Res. Tokyo Series E (36), 1–69.

Iwami, T., Kock, K.-H., 1990. Channichthyidae. In: Gon, O., Heemstra, P.C. (Eds.), Fishes of the Southern Ocean. J.L.B. Smith Institute of Ichthyology, Grahmstown, South Africa, pp. 381–399.

Kishino, H., Hasegawa, M., 1989. Evaluation of the maximum likelihood estimate of the evolutionary topologies from DNA sequence data, and the branching order in Hominoidea. J. Mol. Evol. 29, 170–179.

Kocher, T.D., Conroy, J.A., McKaye, K.R., J.R. Stauffer, J., Lockwook, S.F., 1995. Evolution of NADH dehydrogenase subunit 2 in East African cichlid fish. Mol. Phylogenet. Evol. 4, 420–432.

Kock, K.H., 1992. Antarctic Fish and Fisheries. Cambridge University Press, Cambridge.

La Mesa, M., Vacchi, M., Iwami, T., Eastman, J.T., 2002. Taxonomic studies of the Antarctic icefish genus *Cryodraco* Dollo, 1900 (Notothenioidei: Channichthyidae). Polar Biol. 25, 384–390.

Lewis, P.O., 2001. A likelihood approach to estimating phylogeny from discrete morphological character data. Syst. Biol. 50, 913–925.

Maddison, D.R., Maddison, W.P., 2000. MacClade 4: Analysis of Phylogeny and Character Evolution, 4.0 ed Sinauer, Sunderland, MA.

Meyer, A., 1993. Evolution of mitochondrial DNA in fishes. In: Hochachka, P.W., Mommsen, T.P. (Eds.), Biochemistry and Molecular Biology of Fishes. Elsevier Science Publishers, New York, pp. 1–38.

Near, T.J., Porterfield, J.C., Page, L.M., 2000. Evolution of cytochrome *b* and the molecular systematics of *Ammocrypta*. Copeia 2000, 701–711.

Norman, J.R., 1938. Coast fishes. Part III. The Antarctic zone. Discorery Rep. 18, 1–104.

Orti, G., Petry, P., Porto, J.I.R., Jegu, M., Meyer, A., 1996. Patterns of nucleotide change in mitochondrial ribosomal RNA genes and the phylogeny of piranhas. J. Mol. Evol. 42, 169–182.

Pesole, G., Gissi, C., Chirco, A.D., Saccone, C., 1999. Nucleotide substitution rate of mammalian mitochondrial genomes. J. Mol. Evol. 48, 427–434.

Ritchie, P.A., Lavoue, S., Lecointre, G., 1997. Molecular phylogenetics and the evolution of Antarctic notothenioid fishes. Comp. Biochem. Phys. 118A, 1009–1025.

Shimodaira, H., Hasegawa, M., 1999. Multiple comparisons of log-likelihoods with applications to phylogenetic inference. Mol. Biol. Evol. 16, 1114–1116.

Swofford, D.L., 2000. PAUP*. Phylogenetic Analysis Using Parsimony (*and Other Methods), 4.0b4 ed Sinauer Associates, Sunderland.

Vawter, L., Brown, W.M., 1993. Rates and patterns of base change in the small subunit ribosomal RNA gene. Genetics 134, 597–608.

Voskoboinikova, O.S., 2000. Comparative osteology of *Dacodraco hunteri* and its position within the family Channichthyidae (Notothenioidei). Zool. Zh. 79, 321–332.

Voskoboinikova, O.S., 2001. Evolutionary significance of heterochronies in the development of the bony skeletons of the suborder Notothenioidei (Perciformes). J. Ichthyol. 41, 415–424.